5) Gaseous components from Io, requiring higher-than-volcanic temperatures for evaporation from the body, may be fed into a gas torus at the orbit of Io.

6) X-ray emission from the current spots may be expected (*12*).

Note added in proof: Voyager 2 has since confirmed that at least six of the eight spots were still producing plumes 4 months later. The active spots show a strong concentration to the equator (seven being within 30° of it), an effect expected for the present interpretation but not for volcanoes powered by the tides (*13*).

THOMAS GOLD
Center for Radiophysics and Space Research, Cornell University, Ithaca, New York 14853

References and Notes

1. B. A. Smith *et al.*, *Science* **204**, 951 (1979).
2. L. A. Morabito, S. P. Synnott, P. N. Kupferman, S. A. Collins, *ibid.*, p. 972.
3. R. Hanel *et al.*, *ibid.*, p. 972.
4. S. J. Peale, P. Cassen, R. T. Reynolds, *ibid.* **203**, 892 (1979).
5. In terrestrial volcanic eruptions, dust is often carried to great heights by the buoyancy of hot gases in the atmosphere, an effect that would be absent on Io. High-speed ejection of steam has been observed in terrestrial outbursts, with speeds of ~ 500 m/sec, and rock projectiles thrown from volcanoes ("volcanic bombs") are found at distances that imply ejection speeds of 100 m/sec. The speed of sound in water vapor at a temperature of 1500 K is 930 m/sec [A. Rittman and E. A. Vincent, *Volcanoes and Their Activity* (Wiley, New York, 1962), pp. 38 and 44; S. Self, L. Wilson, I. A. Nairn, *Nature (London)* **277**, 440 (1979)].
6. F. Press and R. Siever, *Earth* (Freeman, San Francisco, 1974), p. 331.
7. N. F. Ness, M. H. Acuña, R. P. Lepping, L. F. Burlaga, K. W. Behannon, F. M. Neubauer, *Science* **204**, 982 (1979).
8. P. A. Cloutier, R. E. Daniell, Jr., A. J. Dessler, T. W. Hill, *Astrophys. Space Sci.* **55**, 93 (1978).
9. A. J. Dessler and T. W. Hill, *Astrophys. J.* **227**, 664 (1979).
10. A detailed estimate of the conductivity of Io as a function of depth cannot be made at this stage. The electrical properties of rocks cover a very wide range, and the composition of Io is not known. All that is necessary for the present discussion is to see that the electrical pathway discussed here would be favored. The interior of Io, if it is liquid rock, would be expected to have a conductivity of at least 10^{-2} ohm^{-1} cm^{-1} (the terrestrial value at a depth of 600 km). A current of 5×10^6 A would then provide a potential drop across the body of the order of 1 V only, a negligible amount compared with the voltage in the circuit of 2×10^5 V (*7*). A cold crust might have a conductivity of 10^{-10} ohm^{-1} cm^{-1} (representative of dry cold rocks) and at a thickness of 50 km would then have a total resistance of 0.3 ohm. A hot pathway through an area of 10 km^2 of the crust, with a conductivity of 10^{-2} ohm^{-1} cm^{-1}, has a resistance of 0.005 ohm and would thus take 60 times the current that would flow diffusely through the crust. These values show that the range of conductances through crust and core that can be expected would favor a current flow through hot spots in the crust and through the core, over an ionospheric path or over a diffuse flow through the crust.
11. Contact resistance arises from the various dissipative effects at such an interface. The kinetic energy of the plasma charge carriers is dissipated there, and the emission of charge from the solid consumes energy, some of which is left in the surface layers.
12. Suggestion by D. Soter (private communication).
13. A. J. Dessler, private communication.
14. I am grateful for discussions with S. Soter and S. F. Dermott.

5 July 1979

Melting of Helium at Room Temperature and High Pressure

Abstract. *Helium has been solidified at room temperature. The melting pressure at 24°C is 115 kilobars, in complete agreement with the Simon equation. An original apparatus was developed for this experiment, which allows loading of the cell at room temperature. Applications to various areas of research are suggested.*

Within the last 10 years, significant progress has been achieved in very high pressure technology (*1*). This progress has been largely due to improvements in the design of pressure generators (*2*) and in measurement procedures (*3*), based on the use of diamond anvil cells which now can be used into the megabar range. Recently (*4*), diamond anvil cells were used in the study of gases; liquid hydrogen was introduced into a diamond anvil cell with a cryogenic setup, and solidification of fluid hydrogen was observed at 57 kbar and room temperature. In this report, we describe a different method in which the cell is loaded at room temperature under a gas pressure of 2000 bars. We could thus measure the melting point of helium (^{4}He) at 24°C and compare it with the melting temperature predicted by existing melting laws. We also found that solid helium may be used as an inert and plastic pressure-transmitting medium for very high pressure research in the diamond cell.

Figure 1 is a sketch of the apparatus that was designed for the experiment.

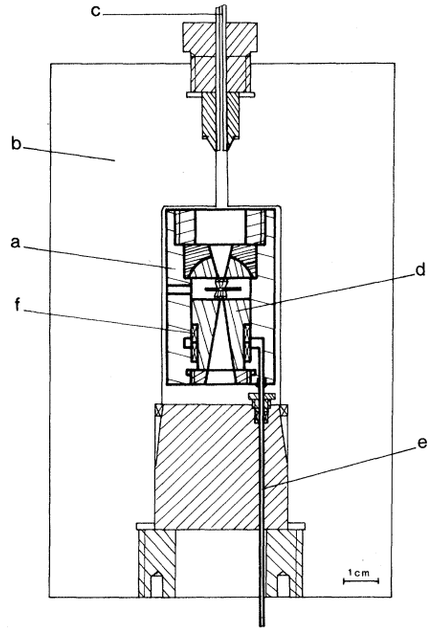

Fig. 1. Sketch of the diamond cell (dark lines) inside the low-pressure vessel (light lines): a, diamond cell (maraging steel); b, low-pressure bomb (5 kbar) (maraging steel, 52RC); c, stainless steel gas-loading capillary; d, moving piston; e, stainless steel capillary feeding the pressure control fluid (helium in this experiment); and f, piston seal.

The diamond anvil cell (a, heavy lines) is contained inside a low-pressure (5-kbar) vessel (b, light lines). At this stage, the diamonds are not pressed against the Inconel gasket. The gas to be studied, helium under a pressure of 2 kbar, is then introduced into bomb b through tubing c. It fills the volume inside the low-pressure bomb, including the sample space between the diamonds and the gasket.

To close the cell, a small overpressure (300 bars) is exerted on piston d, which supports the moving anvil. The necessary pressure, 2300 bars, is fed through capillary e. The resulting force is about 300 kg on ram d, which has a surface area of 1 cm^2. The pressure is sufficient to press the diamonds into the gasket and bring the pressure on the ^{4}He sample up to about 100 kbar. Both pressures controlled through tubings c and e are then decreased from 2000 and 2300 bars, respectively, to 0 and 300 bars, maintaining a difference of 300 bars throughout the whole process. Bomb b can then be opened and the cell extracted with the gas sample still contained between the diamonds.

One can use the cell for optical experiments under variable pressure by changing the pressure on piston d through the capillary e, which is still attached to the cell. The internal pressure is measured on the Ruby fluorescence scale.

The gas used here is U-grade ^{4}He with a nominal impurity content of less than 30 parts per million. Its melting upon slow decompression was directly observed and photographed at the crystal-fluid equilibrium point.

This particular experiment was designed so that we could observe the melting point of helium at around 100 kbar. Thus the dimensions of the anvils, holes, and seats (Fig. 1) that we used would not be suitable for pressures above 200 kbar. At higher pressures, we use a sturdier geometry for the anvils, although the dimensions of the cell remain the same (31 mm in outside diameter and 57 mm long).

Figure 2, a to d, shows the melting process of helium at room temperature (24°C). The two dark objects, near the center and at 4 o'clock, are ruby chips. The diameter of the hole is 130 μm.

Figure 2a shows the solid phase. Grain boundaries between individual microcrystals appear as an irregular network. In Fig. 2b, two crystals are present in the

0036-8075/79/1130-1073$00.50/0

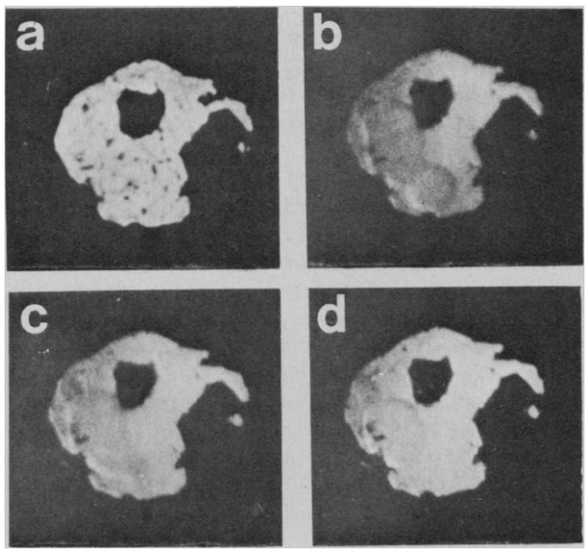

Fig. 2. Melting of helium crystals at room temperature. The total diameter of the cell is 130 μm. The two dark spots near the center and on the right are ruby chips. (a) Solid helium microcrystals fill the entire volume of the cell. (b) During melting, two crystals (lower part, left) are in equilibrium with the fluid. (c) Two minutes later, the smaller crystal has disappeared. (d) Two minutes later than (c), the larger crystal has melted significantly (corners are rounded off). The whole melting process took 10 minutes in this experiment. The total mass of helium was about 0.5 μg.

fluid. The smaller one, with rounded-off edges, melts first and has disappeared in Fig. 2c. In Fig. 2d, the melting process is almost over. The pressure measured at melting is 115 ± 2 kbar at 297 ± 0.4 K (24°C).

The optical contrast between the solid and fluid phases is weak. The refractive indices of both phases are almost the same and presumably very close to unity. With normal illumination, no details were visible. The photographs in Fig. 2 could be taken only with light reflected from the cell walls, at nonnormal incidence.

Melting curves can frequently be represented by the Simon equation, which holds well for rare gases. The pressure P and temperature T at the melting point are related by an exponential law of the form

$$P = aT^c + b$$

where a, b, and c are parameters that are determined by experiment for a given element or compound. Those parameters have been determined by experiments up to 10 kbar and 60 K for helium (*5*). The use of this law up to liquid nitrogen temperature does indeed predict the observed pressure (14 kbar) (*6*). No measurements have been reported above this point, and legitimate questions have been raised on the validity of the Simon equation at very high densities (*5*). The law appears to hold remarkably well even under these conditions. The predicted pressure at 24°C is 115 kbar. For ^{4}He, at least, there does not seem to be a need for a more complicated equation, as was correctly noted from experiments up to 10 kbar (*5*). The calculated density of helium at 115 kbar is about 1.0 g/cm^2.

This verification of the Simon equation up to 115 kbar justifies its extrapolation far above this pressure, except for a phase transition. This regular behavior very strongly points to the retention by solid helium of its 1000-bar structure, which is face-centered cubic. Moreover, a different structure some 50 or 100 kbar above the 115-kbar point is also unlikely since it would be announced by a measurable deviation from the Simon equation (*7*).

This law is applicable to other rare gases. Their melting curves are similar, at high densities, when expressed in "reduced" units to pressure and temperature (*5*, *7*). According to this law, the law of corresponding states, a pressure of 115 kbar for helium is equivalent to a pressure of 575 kbar for argon. The melting behavior of argon and other rare gases is thus known indirectly, at much higher pressures and temperatures, that is, under conditions that are, for the present time, outside experimental possibilities. The reduced pressure range which is now known for helium is 50 times larger than the range where argon was actually measured. This discussion is valid, of course, only in the range where rare gas solids retain their low-pressure, insulating structures. Deviations from it are expected when they transform to a metallic phase.

Dense fluids of any kind can thus be studied in the diamond anvil cell, whether the loading is done by cryogenic methods or high-pressure procedures. Many fields of research may take advantage of this diamond cell.

Theories of melting require experimental data not only on the P-T curves but also on the densities, volume variations on melting, and latent heat. These quantities can either be directly measured or derived by experiments in the diamond cell, along with other physical measurements such as optical absorption or Raman scattering.

Information on the behavior of gases at high densities, especially hydrogen, helium, and their mixtures, is required in many areas. For example, existing models for the interiors of Jupiter or Saturn rely on assumptions about the behavior of the solid and fluid phases of hydrogen and helium. Direct measurements of those elements and their mixtures are now possible up to about 1 Mbar and a few hundred degrees kelvin, which corresponds to depths of a few thousand miles below the visible surface of Jupiter.

Another field where equations of state and phase behavior are useful is laser implosion methods for controlled fusion research. With diamond anvils, the temperatures and pressures that may be attained are much smaller than those that are achieved in these processes, except in some initial stages of implosion. But since the actual conditions must be extrapolated by calculations, the precision of those extrapolations may be increased if one uses improved equations of state, based upon an extended range of experimental data.

Another research area that will benefit from this type of experiments is the study of the metallic state in gases. Prime candidates are hydrogen and its isotopes and the heavier rare gases (krypton and xenon). There are indications that xenon may well reach the metallic state in the vicinity of 300 kbar (*8*), and that hydrogen undergoes the transition somewhat above 1 Mbar. Direct observation of those phases and measurements in the diamond cell will certainly provide greater insight into the mechanism of the transition.

Apart from the consequences for fundamental research, the use of helium in diamond anvil cells may improve very high pressure techniques. It may make it possible for one to circumvent three complicating factors that are commonly encountered when one uses "liquid" pressure media, such as ethanol-methanol mixtures, in research on crystals:

1) These mixtures are very hard glasses above 100 kbar, and stress gradients within the cell cause large pressure inhomogeneities.

2) These mixtures tend to revert to the crystalline state when heated under high pressure, since they are metastable glasses above 20 kbar. They then crystal-

lize in a diffusing and opaque array of microcrystals, precluding optical measurements.

3) They are not inert chemically, especially at the high temperatures (1000 to 2000 K) that are obtainable in the diamond cell and that are necessary for many geophysical problems.

We measured the profile of the ruby luminescence lines up to 150 kbar in solid helium and could see no measurable broadening that would indicate pressure inhomogeneities within the cell. Although this must be checked at higher pressures, it is an indication that helium behaves as a rather "soft" crystal and may well counter the first factor. Concerning the second factor, we could verify (Fig. 2a) that the presence of helium microcrystals does not prevent optical measurements in the cell. Diffusion on grain boundaries is kept at a low level because of the low refractive index of the solid. In other measurements we found it straightforward to crystallize helium in the cell, as a single crystal with no diffusion at all. This would certainly be true at all temperatures, in contrast to metastable ethanol-methanol mixtures. With respect to the third factor, helium is known to be remarkably inert and would probably be the best pressure-transmitting medium, in that respect, for solid-state studies (*9*).

J. M. BESSON
J. P. PINCEAUX
Laboratoire de Physique des Solides, Centre National de la Recherche Scientifique, and
Département des Hautes Pressions, Université Pierre et Marie Curie, 4, Place Jussieu, Tour 13, E2, 75230 Paris, Cedex 05 France

References and Notes

1. S. Block and G. Piermarini, *Phys. Today* **44**, (Sept. 1976).
2. H. K. Mao and P. M. Bell, *Science* **200**, 1145 (1978).
3. G. J. Piermarini, S. Block, J. D. Barnett, R. A. Forman, *J. Appl. Phys.* **46**, 2774 (1975); H. K. Mao, P. M. Bell, J. W. Shaner, D. J. Steinberg, *ibid.* **49**, 3276 (1978).
4. D. H. Liebenberg, R. L. Mills, J. C. Bronson, L. C. Schmidt, *Phys. Lett. A* **67**, 162 (1978); H. K. Mao and P. M. Bell, *Science* **203**, 1004 (1979).
5. R. K. Grawford and W. B. Daniels, *J. Chem. Phys.* **55**, 5651 (1961).
6. D. W. J. Langer, *J. Phys. Chem. Solids* **21**, 122 (1961).
7. S. M. Stishov, *Sov. Phys. Usp.* **17**, 625 (1975); *ibid.* **11**, 816 (1969).
8. D. A. Nelson and A. L. Ruoff, *Phys. Rev. Lett.* **42**, 383 (1979).
9. J. P. Pinceaux, J. P. Maury, J. M. Besson, *C. R. Acad. Sci. Paris* **B288**, 253 (1979); *J. Phys. Lett.* **40**, L307 (1979).
10. Significant help in the development of the techniques we used came from technical and scientific advice from Drs. S. Block and G. Piermarini at the National Bureau of Standards, Washington, D.C., and from Drs. H. K. Mao and P. M. Bell at the Carnegie Institution of Washington.

11 June 1979; revised 31 July 1979

Interplanetary Dust: Trace Element Analysis of Individual Particles by Neutron Activation

Abstract. *Although micrometeorites of cometary origin are thought to be the dominant component of interplanetary dust, it has never been possible to positively identify such micrometer-sized particles. Two such particles have been identified as definitely micrometeorites since their abundances of volatile and nonvolatile trace elements closely match those of primitive solar system material.*

Micrometeorites are micrometer-sized interplanetary dust particles that enter the earth's atmosphere without melting (*1*). They are collected from the stratosphere by U-2 aircraft (*2*) and are being studied because a significant fraction may be particles from comets (*3*). Comets are volatile-rich bodies which may be well-preserved planetesimals that formed at very low temperatures and have been stored at a great distance from the sun, probably for most of the age of the solar system.

We report here the first use of highly sensitive neutron activation analysis techniques to determine trace element abundances of individual micrometeorites. The two particles analyzed [U2-13A1 (70 by 35 μm) and U2-14A6 (42 by 28 μm)] are among the largest of more than 400 extraterrestrial particles that have been collected during 5 years of U-2 flights and are very close to the largest size (for their composition type) that can enter the atmosphere without suffering melting or partial vaporization. Prior to activation analysis, both particles were subjected to routine morphological and qualitative elemental analysis in optical microscopes and scanning electron microscopes (SEM) with energy-dispersive x-ray (EDX) analysis. In the SEM work, it was necessary to sputter-coat the particles with a 100-Å layer of Pd. The diffraction pattern for particle U2-14A6 (made with a small Debye-Scherrer camera) indicates that the bulk of the particle is composed of amorphous or poorly ordered materials. The only strong lines were from magnetite, a minor phase in the particle. Quantitative EDX analysis of particle U2-13A1 (Table 1) represents an average for the top few micrometers of the particle (about 10 percent of the particle mass) (*4*).

Table 1. Surface composition of particulate matter collected from the stratosphere by EDX analysis in an SEM. Values represent element/silicon ratios (in percent by weight). Particle U2-13A3 is a 7-μm chunk of material which fell from the main mass of particle U2-13A1 during handling.

Element	Particle		Bulk C1 (*6*)
	U2-13A1	U2-13A3	
Na	0.25*	0.10	0.098
Mg	0.84	0.87	0.890
Al	0.11	0.12	0.099
S	0.86	0.28	0.53
Ca	0.11	0.10	0.10
Ti	0.006		0.005
Cr	0.023	0.025	0.019
Mn	0.030	0.024	0.017
Fe	2.97	2.12	1.72
Ni	0.15	0.11	0.091

*"Laboratory weathering" is probably responsible for the high Na value (Na tends to migrate toward the surface of the particle) and for antlerlike growths. A peculiar aspect of particle U2-13A1 was the growth of antlerlike fibers during a 2-year storage period in the laboratory. The horn-shaped structures were not seen in the original photos taken soon after collection.

Both particles are black, opaque aggregates of micrometer- and submicrometer-sized grains. Particle U2-13A1 is porous both because of fine-scale voids between individual constituent grains and because of large open vugs as big as 15 μm across. It is more porous than the most porous meteorites and probably has a density of < 2 g cm^{-3}. Qualitatively, both of the particles have essentially chondritic compositions and may be classed as chondritic aggregate interplanetary dust particles, the most common type of micrometeorite (*2*).

The results of neutron activation analyses (*5*) for the two particles are shown in Table 2. Because there is some uncertainty in estimating the weight of these particles, the observed elemental contents are reported as such without converting into concentrations. The concentration of these elements in C1 chondrites (a group of primitive, chemically undifferentiated meteorites that best represent the cosmic or solar system abundance of chemical elements) is also given (*6*). Relative abundances of all the elements except Au in the stratospheric particles are very similar to those of C1 chondrites (*7*). Relative to C1 chondrites, the mean abundances of six nonvolatile elements (Fe, Ni, Cr, Co, Sc, and Ir) in these two particles are 7.33×10^{-8} and 10.5×10^{-8}. If these particles are of C1 composition, then the corresponding weights of 0.07 and 0.11 μg are in good agreement with those inferred from the particle size. The abundance patterns of the particles closely match those of primitive C1, C2, and C3 carbo-

0036-8075/79/1130-1075$00.50/0